FORCE REFLECTING TELEOPERATION WITH ADAPTIVE IMPEDANCE CONTROL [i]

Lonnie J. Love
Robotics and Process Systems Division
Oak Ridge National Laboratory*
Oak Ridge, TN. 37831-6304

Wayne J. Book
School of Mechanical Engineering
Georgia Institute of Technology
Atlanta, GA. 30332-0405

Abstract

Experimentation and a survey of the literature clearly show that contact stability in a force reflecting teleoperation system requires high levels of damping on the master robot. However, excessive damping increases the energy required by an operator for commanding motion. The objective of this paper is to describe a new force reflecting teleoperation methodology that reduces operator energy requirements without sacrificing stability. We begin by describing a new approach to modeling and identifying the remote environment of the teleoperation system. We combine a conventional Multi-Input, Multi-Output Recursive Least Squares (MIMO-RLS) system identification, identifying in real-time the remote environment impedance, with a discretized representation of the remote environment. This methodology generates a time-varying, position dependent representation of the remote environment dynamics. Next, we adapt the target impedance of the master robot with respect to the dynamic model of the remote environment. The environment estimation and impedance adaptation are execute simultaneously and in real time. We demonstrate, through experimentation, that this approach significantly reduces the energy required by an operator to execute remote tasks while simultaneously providing sufficient damping to ensure contact stability.

i This work was supported, in part, by the Office of Naval Research under Interagency Agreement No. 1866-Q356-A1 with the Oak Ridge National laboratory, managed by UT-Battelle, LLC, for the U.S. Department of Energy under contract DE-AC05-00OR22725, and in part by the Office of Naval Research under Interagency Agreement No. 1866-Q356-A1

I. INTRODUCTION

While force reflecting teleoperation has been an active research topic since the 1950's, only a few researchers have explored the role the master robot impedance has on contact stability and performance. Hannaford and Anderson suggest that when the slave robot is unconstrained, the viscous resistance of the master robot should be light to reduce the load on the operator. However, when the slave robot approaches a constraint surface, prior to contact, the target damping on the master robot should increase to provide stable bilateral teleoperation.[1] Chan explored variation of the master robot impedance based upon sensory information.[2] However, this approach only takes effect after contact with the environment. Another example is the work on adaptive impedance control by De Wit and Brogliato.[3] Their work addresses the difficult problem of adapting the target impedance of a robot operating in diverse environments. However, their strategy focuses primarily on robotic force control applications and not teleoperation.

The focus in this manuscript is the impact impedance adaptation on a master robot can have on the stability and performance of a force reflecting teleoperation system. We begin with a brief description of a force reflecting teleoperation system that consists of a long reach flexible manipulator, serving as the slave, and an impedance controlled master. Preliminary experiments in Section III highlight the general problem. During unconstrained maneuvers, it is preferred to have low damping on the master robot to reduce the forces required by the operator to command motion on the slave. However, stability is compromised during contact tasks unless the damping on the master is increased. Thus, our objective is to formulate a teleoperation methodology that adapts the master robot impedance with respect to the remote environment dynamics. In Section IV, we describe the general approach that consists of merging an MIMO-RLS algorithm, for on-line identification of the remote environment impedance, with a discretized model of the slave robot's

workspace. In Section V, we control the target damping on the master robot as a function of the estimated target stiffness of the remote environment. We conclude with a series of experiments using both the fixed and adaptive impedance methodologies on the same task to quantify the impact impedance adaptation has on the operator.

II. TELEOPERATION SYSTEM

We begin with a brief description of the teleoperation system used in this investigation, shown schematically in Figure 1. The system consists of a master robot scaled to human arm motion and a slave robot that has a workspace approximately 50 times the master robot's workspace. This configuration is representative of teleoperation systems used for space based assembly and nuclear waste remediation.[4] To isolate the operator from the slave environment, the master and slave robots are located in different labs in the same building. This configuration allows the investigators to control the visual, acoustic, and tactile sensations that the operator experiences.

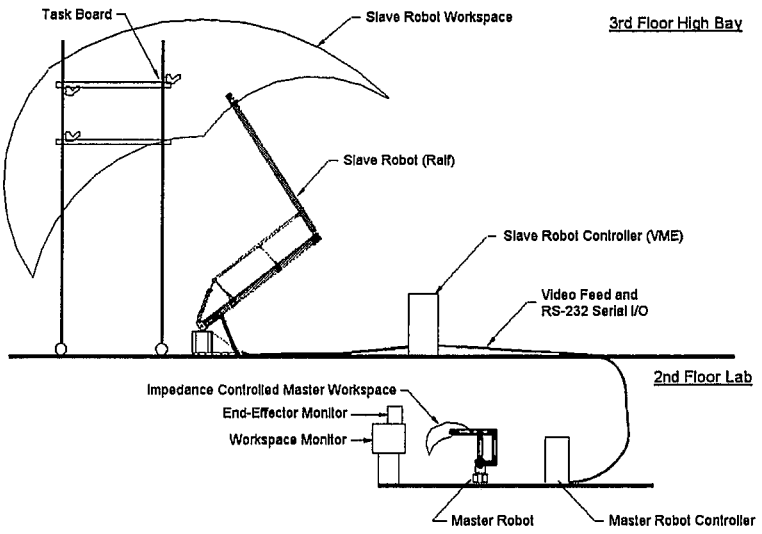

Figure 1: Teleoperation system

The slave robot used in this investigation, shown in Figure 2, is a 2-DOF long reach manipulator. It consists of two cylindrical links with a span of approximately 3-m each and has a

payload capacity of 260-N while its link weight is only 450-N.[5] This manipulator has a low natural frequency (approximately 4 Hz) and damping ratio ($\zeta \approx 0.05$). While not the primary motivation for this research, we will demonstrate how adapting the impedance of a master robot can enable force reflecting teleoperation of flexible manipulators.

Figure 2: Long Reach Manipulator

The master robot, HURBIRT (Human Robot Bilateral Research Tool), is a 2-DOF impedance-controlled robot scaled to human arm motion.[6] To facilitate the teleoperation tasks, the controller for HURBIRT computes and scales its Cartesian tip position from the space of the master robot to the space of the slave, RALF. Currently, 7:1 position amplification permits comfortable mapping of RALF's full workspace into the workspace of the human operator. Once the desired tip position for RALF is calculated, the desired joint position vector is computed and then transmitted to the slave robot's controller. HURBIRT uses a computed torque impedance controller. One example of the target impedance of the master robot is illustrated in Figure 3. The target impedance of the master robot, using the same philosophy of superimposing impedance described by Hogan, is augmented with virtual walls (hashed lines in the figure) that constrain the operator from

commanding the slave robot outside it's workspace.[7] The target impedance for the master robot is defined in Equation (1).

$$M_t\ddot{x} + B_t\dot{x} + F_{vf} + \frac{1}{A}F_e = F_h \tag{1}$$

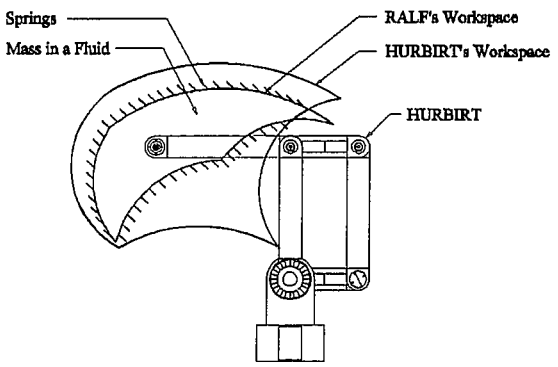

Figure 3: Impedance Controlled Master Robot

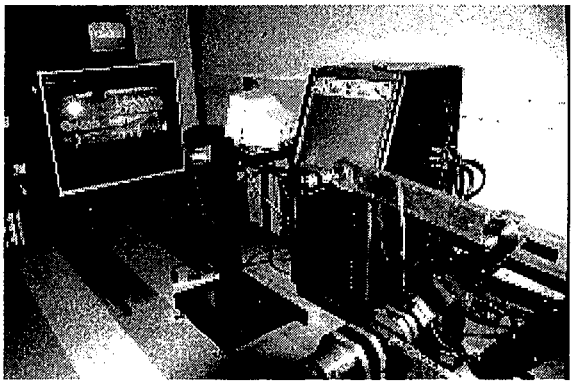

Figure 4: Master Robot Control Station

The mass and damping matrices, M_t and B_t respectively, control the ease with which the operator moves the master robot. The two external stimuli to the master robot include the human applied force, F_h, and the interaction force between the slave robot and its environment, F_e. The scale, A, is the force amplification between the master and slave robots. An additional virtual force, F_{vf}, represents the repulsive force produced by deforming the virtual fixtures, in this case stiff walls constraining the effective workspace of the master robot. Equation (2) provides a model of HURBIRT's dynamic equations of motion with respect to the generalized coordinates, q. This model includes the inertial matrix, D(q), the gravitational load, $\phi(q)$, and the damping and nonlinear velocity terms, $C(q,\dot{q})\dot{q}$. Forces applied to the robot include the joint torque, τ, and the human applied force, F_h, projected to the generalized coordinates through the transpose of the Jacobian, J(q).

$$D(q)\ddot{q} + C(q,\dot{q})\dot{q} + \phi(q) = \tau + J^t(q)F_h \tag{2}$$

The role of the master robot is to provide position commands to the slave manipulator as well as provide force feedback from the remote environment. The computed torque control law in Equation (3) provides the torque compensating for the robot's natural dynamics as well as providing the target impedance in Equation (1). Estimates of the mass properties are denoted by a carat above the symbols. More details regarding the impedance controller for the master robot can be found in [8].

$$\tau = \hat{D}(q)\,J^{-1}(q)\left\{\hat{M}_t^{-1}\left[F_h - \frac{1}{A}F_e - F_{vf} - \hat{B}\dot{x}\right] - \dot{J}(q)\dot{q}\right\} + \hat{C}(q,\dot{q})\dot{q} + \hat{\phi}(q) - J^t(q)F_h \tag{3}$$

In this manuscript, we compare the performance of a fixed and adaptive teleoperation control strategy. We use a single, well-defined task that consists of both unconstrained and contact components along with the transition between these two modes to highlight contact stability. A vertical board, representing a wall in the remote environment, is attached to the task board in the slave robot's workspace. Markers on the wall indicate a path the operator is to follow during the execution of the teleoperated task. Furthermore, the operator is instructed to maintain constant pressure on the wall while moving along this path. The operator begins the task by moving the slave robot from its home position to the top of the wall. After contact is established, the operator moves vertically down the surface of the wall while trying to maintain a constant contact force. After completing the path, the operator maneuvers the robot back to the home position. When the operator starts the task, an array of task execution information (including the task execution time, the power provided by the human to the master robot, and the net interaction force at the tip of the slave and master robot) is recorded for performance assessment.

III. Stability of Bilateral Teleoperation with Link Compliance

Figure 5 illustrates a simplified block diagram of the teleoperation system. For our stability analysis, we truncate the model of the flexible manipulator/controller and only include the first mode of vibration. RALF's first natural frequency is 4.5 Hz with a damping ratio of approximately 0.05. This is approximated by a second order system with a mass of 5.7 kg, viscous damping of 17 $N\text{-}m^{-1}s$ and stiffness of 5000 N/m. In the following experiments, the environment has a stiffness of approximately 2000 N/m. Furthermore, the master robot has a target mass of 10 kg. Figure 6 illustrates the locus of the system's closed loop poles as the target damping of the master robot, B_t, increases from zero to infinity. First, it is clear that for low damping, the system is unstable. Second, increasing the target damping of the master robot moves the unstable poles into the left-half complex plane. It is clear that, while the poles are stable, they are still lightly damped suggesting that vibration will still exist during contact. In addition, as the environment stiffness increases, higher target damping of the master robot is required. This exercise is not intended to predict instability as much as illustrate trends in the systems stability based upon the master robot's target impedance.

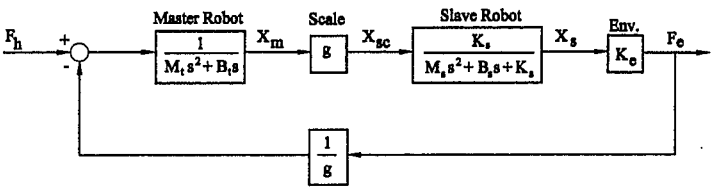

Figure 5: Simplified teleoperation block diagram

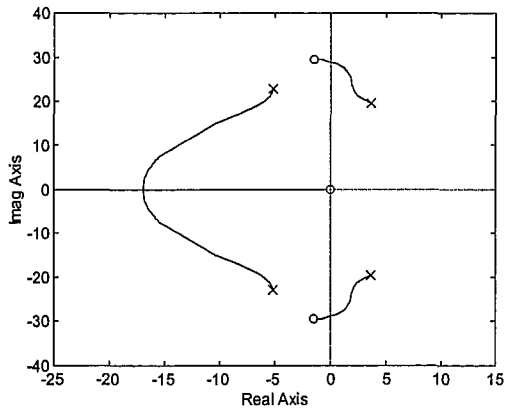

Figure 6: Locus of closed loop poles varying B_t

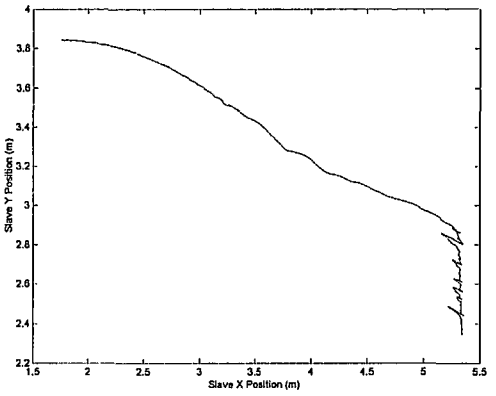

Figure 7: Slave motion during teleoperation with low master damping

The first force reflecting teleoperation experiment has constant target impedance on the master robot with high target damping to ensure stability during contact with the environment. The target impedance in Equation (1) has a 10-kg diagonal mass matrix with a 167 N-m^{-1}s diagonal damping matrix. After 20 repetitions of the task, the mean energy (per task) provided by the opeartor to the master robot is 148 J with a variance of 11.8 J. Likewise, the mean integrated force at the slave robot is 129.9 N-s with a variance of 8.9 N-s. The average slave velocity during unconstrained motion was 0.23 m/sec, reducing to 0.04 m/sec during contact. While high damping ensures stability during contact, it increases the effort an operator must exert during task execution. Lower master damping reduces this effort, but the stability analysis suggests, and experiments show in Figure 7, that low master damping can potentially drive the force reflecting teleoperation system unstable. In this experiment, the operator was unable to maintain contact with the vertical wall (located at the horizontal position X=5.3 m), as illustrated in Figure 7. This provides the motivation for adapting the master robot's damping to variations in the slave's environment impedance.

IV. Remote Environment Estimation

Incorporating an estimate of the remote environment dynamics into the master robot's control structure permits controlling the coupled dynamics between the robot and environment. As with any adaptive control strategy, real-time adaptation of the target impedance of the master robot based upon an estimate of the remote environment's dynamics eliminates the limitations imposed by robust control designs. Unfortunately, estimation of the remote environment is not a trivial task. The remote environment impedance is position dependent, nonlinear and possibly time varying. We present a new method of estimating the dynamics of a robot's environment. This method consists of two fundamental components. First, an MIMO-RLS estimation routine, identifying the relationship between the slave robot's position and tip force sensor data, provides a localized estimate of the environment coupled to the end-effector of the remote robot. Second, a discretized model of the robot's workspace provides a position dependent representation of the remote enviroment impedance. The results of the MIMO-RLS algorithm are stored in an array (the discretized model) whose index corresponds to the tip position of the robot. This combination of the MIMO-RLS and discretized workspace provides a position dependent representation of the environment's dynamics. In addition, a weighted average of the stored estimate with current estimation results provides a method of tracking time dependent variations in the environment. For brevity, we refer the interested reader to [9] for details on the MIMO-RLS and [8] for details on it's implementation in this investigation. The primary input to the MIMO-RLS algorithm is the force and position of the slave manipulator and the output is time varying mass (M), damping (B), and stiffness (K) matricies.

If, during the execution of a task, a robot departs from a region, then moves back, the transients associated with the estimation process are repeated and delay the convergence of the environment estimate. Providing position dependent memory of the estimated environment

dynamics minimizes these transient effects. One approach to providing a position dependent model of a robot's environment is to discretize the robot's workspace into many discrete cells. Each of these cells represents a small volume of the robot's workspace. After each cycle of the estimation process, the updated parameters of the environment model are stored in the cell that corresponds to the current tip position of the robot. Figure 8 illustrates an example of the workspace of a robot discretized by a finite number of cells.

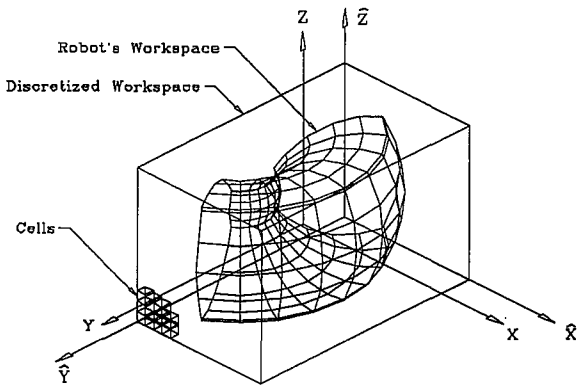

Figure 8: Discretized Workspace

The volume of the discretized workspace is bounded by the limits of the robot's motion. These limits are generalized into extremums of the robot's travel with respect to the cartesian coordinate system, XYZ. If the size of these cells is uniform, the volume of the discrete cells is dependent upon the volume of the robot's workspace and the number of cells allocated for the workspace.

$$V_{cell} = \frac{(x_{max} - x_{min})(y_{max} - y_{min})(z_{max} - z_{min})}{N_x N_y N_z} \tag{4}$$

where N_x, N_y, and N_z represent the number of cells allocated along the X, Y, and Z axes respectively. A second coordinate system, $\hat{X}, \hat{Y}, \hat{Z}$, has its origin at the minima of the robot's workspace.

$$\hat{x} = x - x_{min}$$
$$\hat{y} = y - y_{min} \qquad (5)$$
$$\hat{z} = z - z_{min}$$

The index of the cell, defined below in Equation (6), provides a position dependent relationship between the tip position of the robot and the index of the array representing the robot's workspace.

$$n_x = \text{int}\left(N_x \frac{x - x_{min}}{x_{max} - x_{min}} \right)$$
$$n_y = \text{int}\left(N_y \frac{y - y_{min}}{y_{max} - y_{min}} \right) \qquad (6)$$
$$n_z = \text{int}\left(N_z \frac{z - z_{min}}{z_{max} - z_{min}} \right)$$

The slave robot's planar workspace, in our example, is approximately 10 square meters. To provide high resolution without excessive memory requirements, the workspace is discretized as a 100 x 100 array. Each element of the two dimensional array corresponds to one square centimeter of the master robot's workspace. Environment parameters generally vary with position. The current model of the robot's environment assumes that this variation is fixed across the space of each cell. The tip position of the slave robot, $x \in R^2$, is transformed to a coordinate system defined within the space of the corresponding cell. This coordinate system, $(u,v) \in [0,1]x[0,1]$, provides a normalized representation of the tip position of the robot within the space of the cell. The basis function for this model of the environment provides a constant distribution, $\phi(u,v) = 1$, across the surface of the cell. There may be an advantage to providing nonuniform basis functions across the surface of each cell. To smooth, spatially, the transition between cells, we apply a Bezier approximation between coincident cells.[8] To provide memory of past estimation results, a weighted average of the latest estimate and previous results is stored in the cell. This is accomplished by first extracting the stored

results out of the current cell location. This past average is weighted and updated with the current results. Consider the stiffness matrix, $\hat{K}$, in Equation (7).

$$\hat{K}(n_x, n_y)[k] = w\, K(n_x, n_y)[k] + (1 - w)\, \hat{K}(n_x, n_y)[k-1] \tag{7}$$

The matrix K[k] (small k is the sample time index) is the current estimate of environment stiffness from the MIMO-RLS algorithm. $\hat{K}(n_x, n_y)[k-1]$ is the previous estimate of the stiffness matrix stored in the (n_x, n_y) cell. Note the carat to destinguish between the RLS estimate, $K(n_x, n_y)$, and the stiffness stored in the discretized workspace, $\hat{K}(n_x, n_y)$. The weight, w, should be a value between zero and one. If the value is small, the latest update of the environment has little effect on the stored results in the cell. If the weight is close to one, the value in the cell is greatly influenced by the latest results. A value of w=0.25 was used for this investigation. Figure 9 is a graphical depiction of the identification algorithm where z is the sample delay operator.

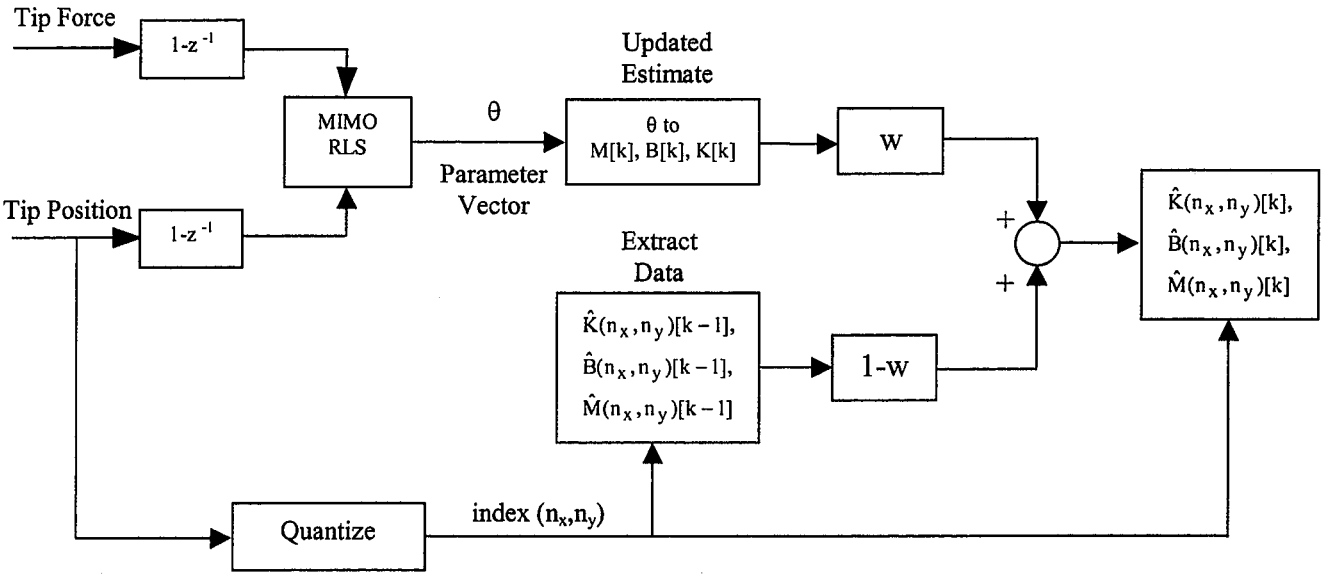

Figure 9: Flow Chart for Environment Estimation

V. REMOTELY ADAPTING IMPEDANCE CONTROL

Focus now shifts to the adaptation of the target impedance of the master robot based upon the above on-line estimation of the remote environment coupled to a slave robot. The damping matrix, B_t, is the target impedance of the master robot is defined in Equation (1). The damping ratio, ζ_t, is set to 1.0 to minimize vibration during contact with the environment. The index n_x and n_y correlate the tip position of the master robot to the discretized workspace and subsequently the elements of the localized stiffness matrix of the remote environment, $\hat{K}(n_x,n_y)$.

$$B_t = 2\zeta_t\sqrt{M_t\hat{K}(n_x,n_y)} \tag{8}$$

High environment impedance is assumed when the operator maneuvers the slave robot into a region where high uncertainty exists in the environment estimation. Each cell is initialized with a stiffness of 700 N/m. This ensures that when the slave robot moves into a new region, the adapted target impedance is the same as the target impedance used in the fixed impedance bilateral teleoperation experiments with B_t=167 N-m^{-1}s. Figure 10 illustrates the resulting K_{XX} stiffness grid after 10 repetitions of the task. The figure clearly shows that there is a region of space in which the estimated environment stiffness is negligible. This region coincides with the unconstrained space that the robot maneuvers through during the execution of the task. As the robot moves through unconstrained space, these cells converge to zero stiffness reducing the target damping of the master robot's impedance controller. Thus, the robot adapts its damping based upon the remote environment impedance. If the operator attempts to maneuver into a new region, the viscous resistance of the master robot increases in concert with the default high environmental stiffness values. Likewise, regions with high stiffness provide higher damping on the master robot.

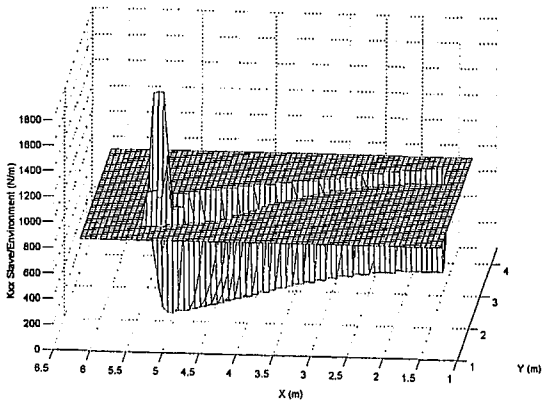

Figure 10: Identified remote environment stiffness

The same series of experiments described earlier are conducted using the adaptive impedance control paradigm. The compliance of the slave robot and environment is evident in the force profiles recorded during the task. Figure 11 shows the tip position of the slave manipulator during the task. Comparing this to Figure 7, it is clear that the increased damping during contact stabilizes the system. Figure 12 and Figure 13 show the external force due to the environment on the slave as well as the human applied force on the master. After the robot contacts the wall, there is a low frequency (< 1Hz) vibration. Due to the force feedback to the master robot, the operator feels this vibration (ripples in Figure 13), but is capable of maintaining contact and completing the task.

We wish to add some general comments regarding this vibration before continuing. During static contact tasks (only maintaining contact, not hybrid contact/motion), no vibration is evident during and after contact. Only during hybrid motion (constrained in one direction, moving in orthogonal direction) does the system exhibits this oscillatory motion. The source of this vibration is still under investigation and could be due to a one or a combination of many factors (calibration errors between the master and slave, phase lag in the joint compensators, compliance of the slave manipulator, nonlinearities in the hydraulic actuation...). There are many details that are lumped

together or neglected in the simplified models used in the stability analysis. However, this vibration should not detract from the fact that a general adaptive teleoperation methodology enables stable force reflecting teleoperation of a system with considerable link and joint compliance. We are unaware of any work in the literature regarding force reflecting teleoperation on a system of comparable size and compliance. Mitigation of this vibration is a continuing area of research.

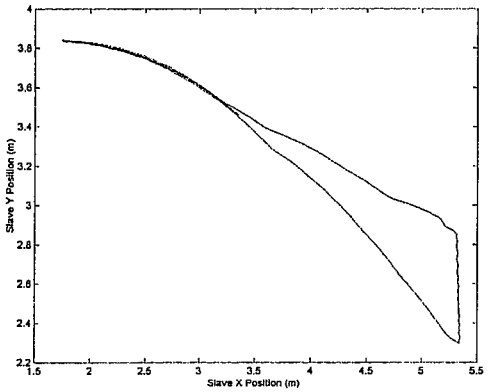

Figure 11: Slave motion with adaptation

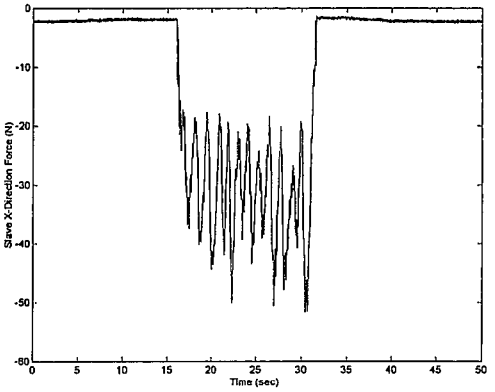

Figure 12: Slave/environment interaction force

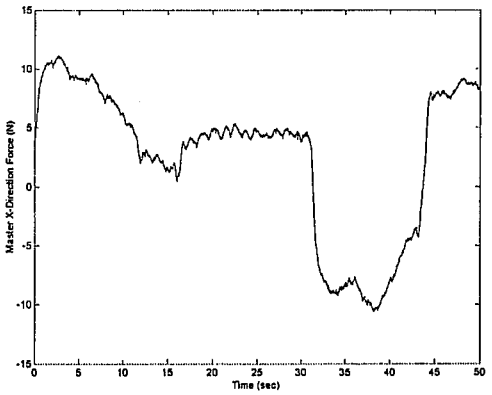

Figure 13: Human applied force

A quantitative comparison of the two bilateral teleoperation systems (fixed impedance and adaptive impedance) provides insight into the advantage of adaptive bilateral teleoperation systems.

The only difference between the teleoperation experiments is the addition of the adaptive damping based upon estimated environment impedance. The initial stiffness of 700 N/m ensures that the adaptive impedance controller has the same target impedance as the fixed impedance when the slave robot maneuvers into a new region. An operator executed the task twenty times, first using the adaptive teleoperation system. Next, the same operator executed the same task 20 times using the fixed impedance teleoperation scheme. Figure 14 and Figure 15 illustrate the task execution time and the integrated force in the remote environment.

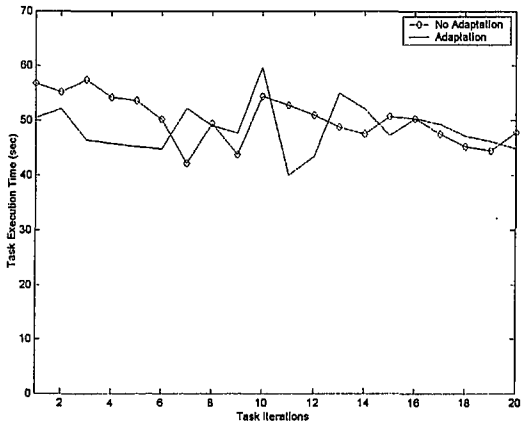

Figure 14: Task completion time

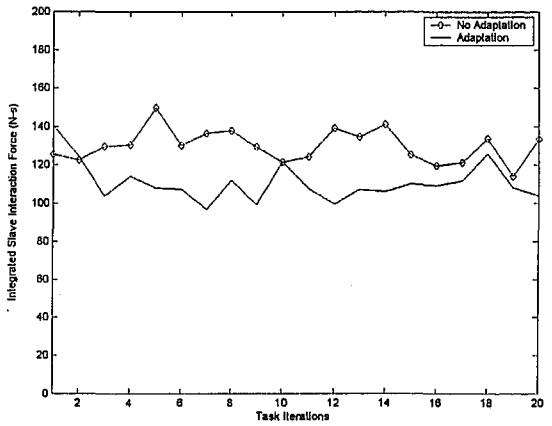

Figure 15: Integrated slave/environment interaction force

From these displays, it appears that the remote task is executed with approximately the same proficiency when using either fixed or adaptive impedance control on the master robot. Figure 16 and Figure 17 compare the human applied energy and the integrated interaction force at the master robot using fixed and adaptive impedance control. A comparison of these figures suggests that less energy and force is required of the human to complete the same task. After 20 repetitions of the task (the identification process generally converges after the second repetition of the task), the mean energy provided by the human to the master robot (per task) is 59.6 J with a variance of 10.1 J. Recall that the operator energy with fixed impedance was 148 J per task. The mean integrated force

at the slave robot (per task) is 124.3 N-s with a variance of 7.9 N-s, which is close to the force level (129.9 N-s) experienced during the fixed impedance experiment. This reduction in energy, which is evident after the first task iteration, reduces the potential for fatigue during teleoperated tasks.

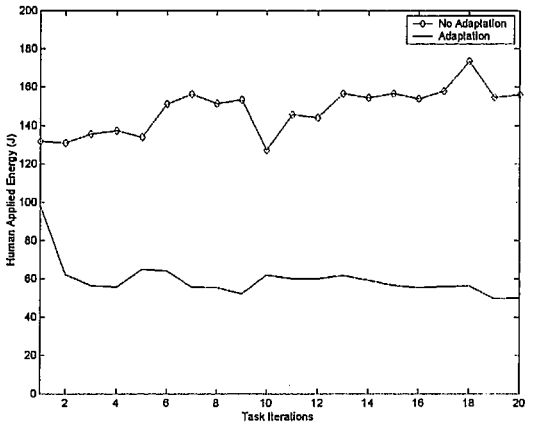

Figure 16: Human applied energy

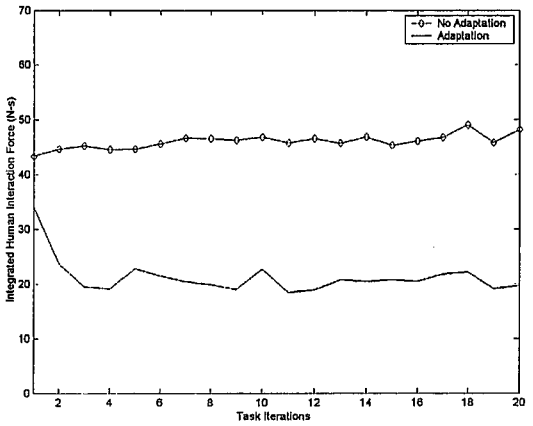

Figure 17: Integrated human/master interaction force

The construction of a position dependent model of the slave robot's environment has one clear advantage over time-based approaches. By including surrounding cells in the impedance adaptation, it is possible to adapt the target damping prior to contact making the adaptation acausal. This has a direct impact on contact stability.

VI. CONCLUSION

This paper describes a novel approach to adapting the impedance of a teleoperation system based on an estimate of the remote environment dynamics. A method for modeling and identifying a slave robot's environment is described. This model provides valuable information that improves the performance of bilateral teleoperation systems. Experiments show that adapting the target damping of the master to variations in the slave robot's environment reduce the operator's energy, and thus reduce fatigue, during the execution of a task.

The teleoperation system used for this investigation utilized a slave manipulator with considerable link compliance. While simple contact tasks demonstrated contact stability, a low frequency vibration persisted during hybrid motion. Future work will focus on methods to suppress this vibration during bilateral teleoperation. In addition, alternative approaches to environment identification may be explored. One of the weaknesses of the approach described in this manuscript is the differentiation of the force signal for computation of environment stiffness. This differentiation proves to be quite noisy. Lee and Asada recently demonstrated environment identification based on the correlation of perturbations and force measurements, resulting in an integration procedure as opposed to differentiation.[10] Another approach may consist of exploiting alternative sensors, such as ultrasonic or vision systems, to correlate obstacles into position dependent models. Future work will explore methods to simplify the identification process to decrease complexity and increase robustness.

ACKNOWLEDGEMENTS

The author would like to state his appreciation to the Intelligent Machines and Dynamics research group at Georgia Tech for their guidance and support. In addition, the first author would like to acknowledge the support of Dr. Theresa McMullen and the Office of Naval Research under Interagency Agreement No. 1866-Q356-A1, whose support made this publication possible.

REFERENCES

[1] Hannaford, B., and Anderson, R., "Experimental and Simulation Studies of Hard Contact in Force Reflecting Teleoperation," *IEEE International Conference on Robotics and Automation*, Vol. I, pp. 584-589, 1988.

[2] Chan,T., Everett,S., and Dubey,S., "Variable Damping Impedance Control of a Bilateral Telerobotic System," *Proceedings of the IEEE International Conference on Robotics and Automation*, pp.2033-2040, 1996.

[3] De Wit, C., and Brogliato, B., "Direct Adaptive Impedance Control Including Transition Phases," *Automatica*, Vol.33, No. 4, pp.643-649, 1974.

[4] S. Kreig, W. Jenkins, K. Leist, K. Squires, J. Thompson, *Single-Shell Tank Waste Retrieval Study*, Westinghouse Hanford Co. Report for the U.S. Department of Energy, 1990.

[5] J. Huggins, D. Kwon, J. Lee, W. Book, "Alternate Modeling and Verification Techniques for a Large Flexible Arm," *Proceedings of the Conference. on Applied Motion Control*, pp.157-164, 1987.

[6] L. Love, and W. Book, "Design and Control of a Multiple Degree of Freedom Haptic Interface," *Proceedings of the ASME-Winter Annual Meeting, Dynamic Systems and Control*, pp. 851-856, 1994.

[7] N. Hogan, "Impedance Control: An Approach to Manipulation," *ASME Journal of Dynamic Systems, Measurement., and Control*,Vol.107, pp.17-24, 1985.

[8] L.Love, "Adaptive Impedance Control," *Ph.D. Thesis*, Georgia Institute of Technology, Atlanta, GA, 1995.

[9] Ljung, L., System Identification: Theory for the User, *Information and Systems Sciences Series*, ed. T. Kailath, Englewood Cliffs, N.J., Prentice Hall, 1987.

[10] Lee, S., and Asada, H., "A Perturbation/Correlation Method for Force Guided Robot Assembly," *IEEE Transactions on Robotics and Automation*, Vol. 15, No.4, August 1999.